

# Transient Behaviour of Two Parallel Connected Flywheel Generators During Pulsed Power Operation

A. M. Miri, V. Landenberger  
University of Karlsruhe, IEH  
Kaiserstr. 12, D-76128 Karlsruhe, Germany  
miri@ieh.etec.uni-karlsruhe.de

C. Sihler, B. Streibl  
Max-Planck-Institut für Plasmaphysik (IPP)  
Boltzmannstr. 2, D-85748 Garching, Germany  
sihler@ipp.mpg.de

**Abstract** - IPP's AxiSymmetric Divertor EXperiment (ASDEX Upgrade) belongs to the tokamak family. The power supply of ASDEX Upgrade comprises the flywheel generators EZ3 (500 MJ / 144 MVA) and EZ4 (650 MJ / 220 MVA). So far, each synchronous machine has been feeding its own 10.5 kV grid. In both grids sudden load changes can occur and the power frequencies may decrease from 110 Hz to 85 Hz. These requirements and the different electrical and mechanical parameters of both generators require detailed numerical models for an investigation of the stability limits of a parallel operation of these machines on one common busbar. In the paper the flywheel generator models derived from analytical calculations and measurements are described and first stability investigations are presented showing the transient behaviour of the two parallel connected flywheel generators during nominal pulsed power operation.

**Keywords:** Transient Analysis, Modelling, Stability, Synchronous Machines, Simplorer

## I. INTRODUCTION

For more than three decades, worldwide efforts have been made to investigate the fusion of the hydrogen isotopes deuterium and tritium for energy production. A number of principles are available for the experimental devices serving this purpose. One of the most favourable is the toroidal confinement of an ionized gas (plasma) which is heated to about 100 million degrees and confined in a vacuum chamber by the field of large magnets. The type of magnetic plasma confinement device, with a high electric current of the order of several  $10^6$  amperes flowing in the plasma, is named tokamak.

The Max-Planck-Institut für Plasmaphysik, Garching, commissioned such a device, called ASDEX Upgrade, in 1991. In this device the ring-shaped hydrogen plasma carries an electric current up to  $1.4 \times 10^6$  A. The magnetically coupled coils of

the experimental device which is shown in Fig. 1 require an electric power of several hundred MVA for about 10 s [1]. Static power converters powered by flywheel generators are used to feed the coils.

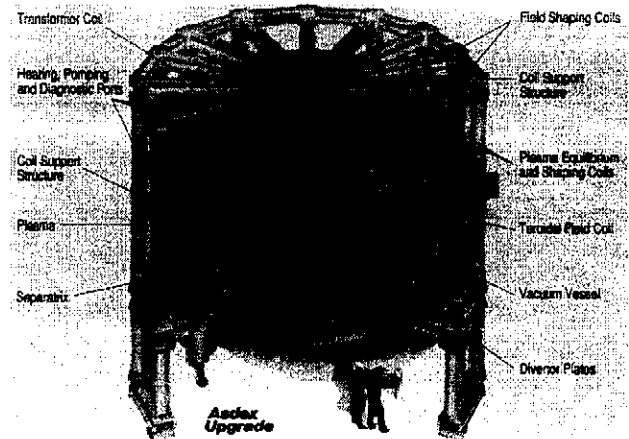


Fig. 1. ASDEX Upgrade tokamak

The time of construction of the flywheel generators EZ3 and EZ4 are ten years apart from each other and the electrical and mechanical properties of the machines are quite different. Therefore, each generator feeds its own 10.5 kV system. For future plasma experiments a parallel operation of both flywheel generators on one common busbar would be favourable.

## II. DERIVATION OF THE FLYWHEEL GENERATOR MODELS

Detailed models are stringent for a stability analysis of the parallel connected flywheel generators because of the pulsed power requirements of ASDEX Upgrade. The course of a load pulse is as follows (generator data see Table 1):

1. Ramping up of the flywheel generators to a predefined r.p.m. value and provision of the nominal voltage (controlled voltage of 10.5 kV).
2. Start of pulse: The active power supplied causes a speed drop of the flywheel generators and a decrease of the grid frequency

3. End of pulse: It takes several minutes to ramp up the flywheel generators to the operating range required for the next pulse (range of operation: 85-110 Hz).

Table 1. Relevant machine data

| Flywheel generator                                       | EZ3                                              | EZA                                              |
|----------------------------------------------------------|--------------------------------------------------|--------------------------------------------------|
| Design voltage                                           | $U_n = 10.5 \text{ kV}$                          | $U_n = 10.5 \text{ kV}$                          |
| Nominal apparent power in pulsed operation               | $S_n = 144 \text{ MVA}$<br>$\cos \varphi = 0.93$ | $S_n = 220 \text{ MVA}$<br>$\cos \varphi = 0.49$ |
| Nominal frequency                                        | $f_n = 100 \text{ Hz}$                           | $f_n = 100 \text{ Hz}$                           |
| Moment of inertia                                        | $J = 90.4 \text{ tm}^2$                          | $J = 120.3 \text{ tm}^2$                         |
| Initial rotational speed                                 | $n = 1650 \text{ min}^{-1}$                      | $n = 1650 \text{ min}^{-1}$                      |
| Unsaturated/saturated synchronous reactance, direct axis | $x_{du} = 4.5 / x_{ds} = 3.6$                    | $x_{du} = 2.63 / x_{ds} = 2.24$                  |
| Unsaturated synchronous reactance, quadrature axis       | $x_q = 3.1$                                      | $x_q = 1.62$                                     |
| Unsaturated subtransient reactance, direct axis          | $x_{du}'' = 0.186$                               | $x_{du}'' = 0.175$                               |
| Unsaturated subtransient reactance, quadrature axis      | $x_{qu}'' = 0.19$                                | $x_{qu}'' = 0.147$                               |
| Unsaturated transient reactance, direct axis             | $x_{du}' = 0.68$                                 | $x_{du}' = 0.328$                                |
| Transient short-circuit time constant                    | $T_d' = 0.55 \text{ s}$                          | $T_d' = 0.204 \text{ s}$                         |
| Subtransient short-circuit time constant                 | $T_d'' = 0.03 \text{ s}$                         | $T_d'' = 0.021 \text{ s}$                        |
| Winding resistance at $T=20^\circ\text{C}$               | $R_l = 5.9 \text{ m}\Omega$                      | $R_l = 2.68 \text{ m}\Omega/\text{Strang}$       |
| Exciter resistance at $T=20^\circ\text{C}$               | $R_f = 83 \text{ m}\Omega/\text{Strang}$         | $R_f = 130.4 \text{ m}\Omega$                    |
| Rated excitation current at minimum rotational speed     | $I_{fm} = 2522 \text{ A}$                        | $I_{fm} = 2568 \text{ A}$                        |

Starting from these data all relevant parameters for the machine models employing "Watcom" ATP and Simplorer [2] were derived analytically. In Simplorer the machine model is based on equation system (1) [3, 4].

$$\begin{aligned}
 u_d &= R_i i_d + \frac{d\psi_d}{dt} - \omega \psi_q & u_{fd} &= R_{fd} i_{fd} + \frac{d\psi_{fd}}{dt} \\
 u_q &= R_i i_q + \frac{d\psi_q}{dt} + \omega \psi_d & 0 &= R_{Dd} i_{Dd} + \frac{d\psi_{Dd}}{dt} \\
 u_0 &= R_i i_0 + \frac{d\psi_0}{dt} & 0 &= R_{Dq} i_{Dq} + \frac{d\psi_{Dq}}{dt}
 \end{aligned}$$

$$\begin{pmatrix} \psi_d \\ \psi_{Dd} \\ \psi_{fd} \end{pmatrix} = \begin{pmatrix} L_d & L_{aDd} & L_{afd} \\ \frac{3}{2} L_{Dad} & L_{DDd} & L_{Dfd} \\ \frac{3}{2} L_{fad} & L_{fDd} & L_{ffd} \end{pmatrix} \begin{pmatrix} i_d \\ i_{Dd} \\ i_{fd} \end{pmatrix}$$

$$\begin{pmatrix} \psi_q \\ \psi_{Dq} \end{pmatrix} = \begin{pmatrix} L_q & L_{aDq} \\ \frac{3}{2} L_{Daq} & L_{DDq} \end{pmatrix} \begin{pmatrix} i_q \\ i_{Dq} \end{pmatrix} \quad (1)$$

$$\begin{aligned}
 \psi_0 &= L_0 i_0 \\
 m &= p \frac{3}{2} (\psi_d i_q - \psi_q i_d) \\
 m + m_A &= J \frac{1}{p} \frac{d^2 \vartheta}{dt^2} \\
 \omega &= \frac{d\vartheta}{dt}
 \end{aligned}$$

- $\Psi_{Dd}, \Psi_{Dq}$ : Flux linkage of d- and q-axis of damper winding
- $i_{Dd}, i_{Dq}$ : Damper winding current (d- and q-axis component)
- $\Psi_{fd}$ : Flux linkage of exciter winding
- $i_{fd}$ : Exciter winding current
- Direct axis inductances:

| Coupling inductance | Stator    | Damper    | Exciter   |
|---------------------|-----------|-----------|-----------|
| d                   |           |           |           |
| Stator              | $L_d$     | $L_{aDd}$ | $L_{afd}$ |
| Damper              | $L_{Dad}$ | $L_{DDd}$ | $L_{Dfd}$ |
| Exciter             | $L_{fad}$ | $L_{fDd}$ | $L_{ffd}$ |

- Quadrature axis inductances:

| Coupling inductance q | Stator    | Damper    |
|-----------------------|-----------|-----------|
| Stator                | $L_q$     | $L_{aDq}$ |
| Damper                | $L_{Daq}$ | $L_{DDq}$ |

- $L_0$ : Zero-sequence inductance
- $\vartheta$ : Instantaneous position of rotor

The dq0 parameters [3 - 5] of equation system (1) were extracted from the machine parameters in Table 1 as outlined in the Appendix.

In continuous operation the nominal apparent power of the flywheel generators EZ3 and EZ4 is one order of magnitude smaller than under pulsed conditions. Therefore, in pulsed operation, both machines are in the saturated state. Whereas in Simplorer the effects of saturation were considered using saturated machine parameters (linear approximation), the ATP simulations are performed using a characteristic curve for saturation.

### III. SIMULATION AND MEASUREMENT OF THE TRANSIENT BEHAVIOUR OF GENERATOR EZ3

Extensive measurements were performed on generator EZ3 to investigate the validity of the Simplorer model (linear approximation of saturation) during pulsed operation. Fig. 2 shows a typical result.

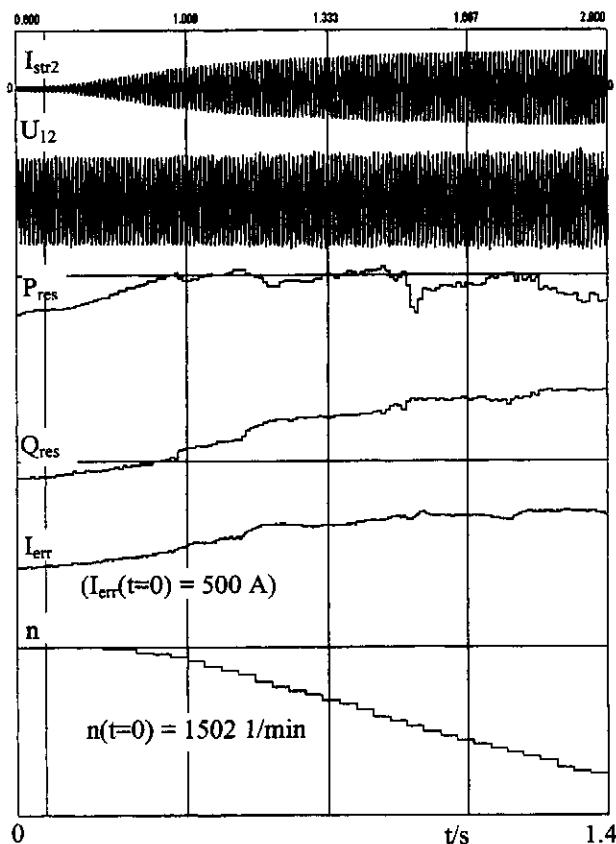


Fig. 2. *Measurement* of characteristic values of generator EZ3 at the beginning of an ASDEX Upgrade pulse with a plasma current of 1 MA

$I_{str2}$ : Phase current [- 8 kA ↔ 8 kA]  
 $U_{12}$ : Phase-to-phase voltage [-18 kV ↔ 18 kV]  
 $P_{res}$ : Active power [- 40 MW ↔ 40 MW]  
 $Q_{res}$ : Reactive power [ 0 ↔ 82 MVar]  
 $I_{err}$ : Exciter current [ - 500 A ↔ 2000 A]  
 $n$ : Rotational speed [1470 ↔ 1530 1/min]

In order to simplify the interpretation of the measurement results only vertical field coils were connected to the flywheel generator EZ3 during the load pulse shown in Fig. 3. Only the beginning of the load pulse is shown: the ramp-up of the plasma and vertical field coil currents to their stationary values during the flat-top phase ( $t > 1.35$  s). The flat-top phase is characterized by a stationary plasma current of 1.0 MA.

During the first second there is a relative high demand of active power which is used in the ASDEX Upgrade tokamak to build up the magnetic fields required for the plasma confinement. That phase is also characterized by a relative steep drop of rotational speed. During the plasma flat-top phase ( $t > 1.35$  s) there is a high proportion of reactive power being generated by the thyristor converters which are necessary for controlling the plasma.

In Fig. 3 the transient behavior of generator

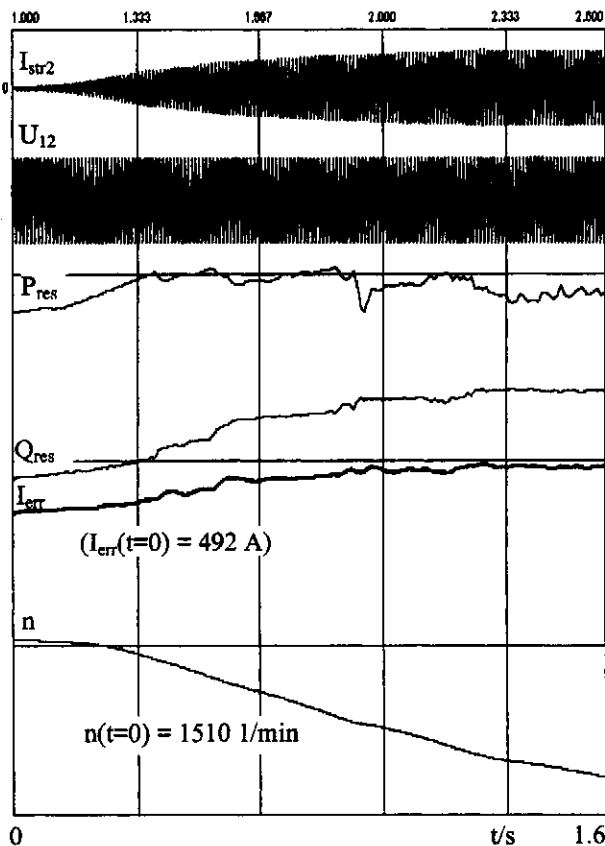


Fig. 3. *Simulation* of characteristic values of generator EZ3 at the beginning of the pulse shown in Fig. 2 employing the Simplorer code

$I_{str2}$ : Phase current [- 8 kA ↔ 8 kA]  
 $U_{12}$ : Phase-to-phase voltage [-18 kV ↔ 18 kV]  
 $P_{res}$ : Active power [- 40 MW ↔ 40 MW]  
 $Q_{res}$ : Reactive power [ 0 ↔ 82 MVar]  
 $I_{err}$ : Exciter current [ - 1500 A ↔ 1500 A]  
 $n$ : Rotational speed [1470 ↔ 1530 1/min]

EZ3 was calculated using the load parameters  $P_{res}$  and  $Q_{res}$  evaluated from the measurement. The good agreement between calculated and measured results was not only achieved during the ramp-up, but also during the flat-top phase.

Since the linear approximation model for saturation effects being used in the Simplorer simulations seems to be sufficiently accurate for simulating the transient behaviour of the generators during pulsed power operation, the same type of model was also used for generator EZ4. With these models preliminary investigations of the stability of the parallel connected generators during pulsed operation were performed.

#### IV. INVESTIGATION OF THE TRANSIENT BEHAVIOUR OF A PARALLEL CONNECTION OF EZ3 AND EZ4

First investigations were performed using the Simplorer code as described in the previous section. The simulations were realized by means of two generators, EZ3 and EZ4, connected to the same busbar. The applied load function is shown in Fig. 4. The power factor of the load varies between  $\cos \varphi = 1.0$  ( $t = 0.5$  s) and  $\cos \varphi = 0.2$  ( $t > 1.5$  s). A simple progression of the load function was assumed to facilitate the interpretation of the results.

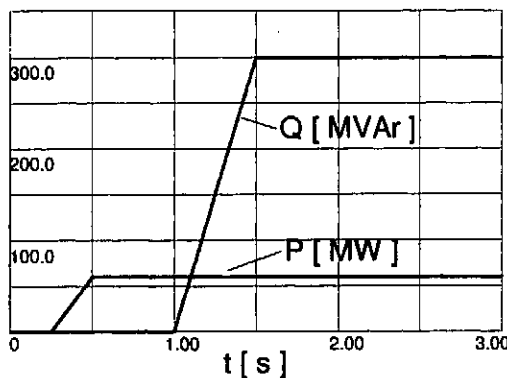


Fig. 4. Impressed load on the two machine system  
P: Active power, Q: Reactive power

Fig. 5 shows the effective load current and the effective generator currents of EZ3 and EZ4. It can be seen that both machines feed the load with power ratios that are about proportional to the nominal powers of the two machines. Fig. 5 also shows that there is no relevant circulating current between the machines. This has been achieved without modifying the control system of the two generators. Only the proportional component of the busbar voltage controller of both machines has been adapted to the new situation.

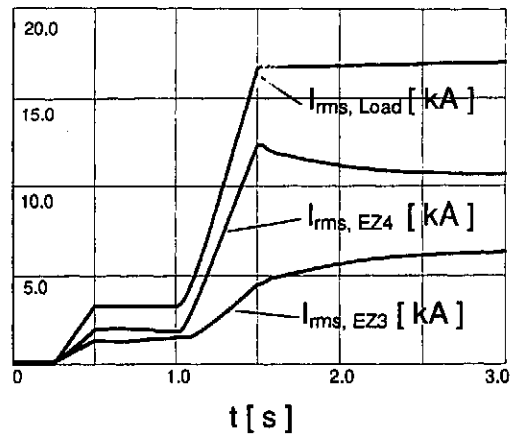


Fig. 5. Effective phase currents with EZ3 and EZ4 in parallel operation (load function see Fig. 4)

One object of further investigations will be the design of a regulating concept to optimize the dynamic response of both machines on sudden load changes.

As both machines are operating on the same busbar, it is obvious that they have nearly the same angular speed, except for asynchronous effects which occur during transient processes. Fig. 6 shows the rotor speed. There is a drop in velocity as well as in the one-machine system. Since both machines are operating inside the same system, they are forced to maintain one common angular speed.

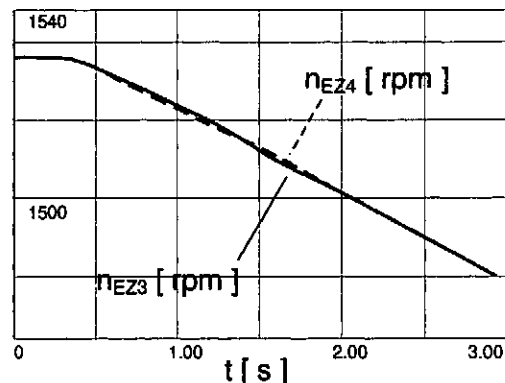


Fig. 6. Rotor speed of EZ3 and EZ4

Focusing on the exciter level, the currents of EZ3 and EZ4 are displayed in Fig. 7. As was expected the steep increase of reactive power causes a steep increase of the exciter currents. Both exciter currents do not exceed their nominal values even though the reactive load increases by 300 MVAR within 0.5 s. A well balanced load distribution is also displayed in Fig. 8 which shows the active and reactive power portions of both machines feeding the impressed load in Fig. 4.

Finally, the stability of the two-generators system is to be investigated. A closer look at the

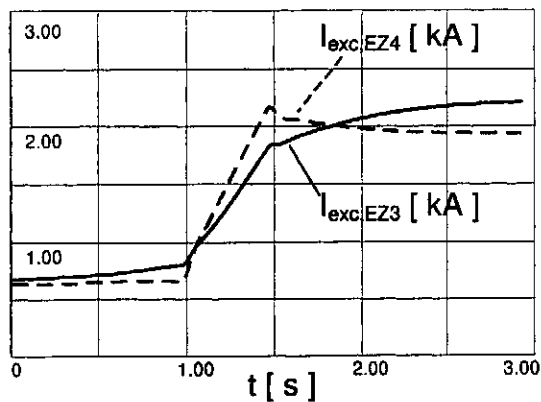


Fig. 7. Exciter currents of EZ3 ( $I_{exc, EZ3}$ ) and EZ4 ( $I_{exc, EZ4}$ )

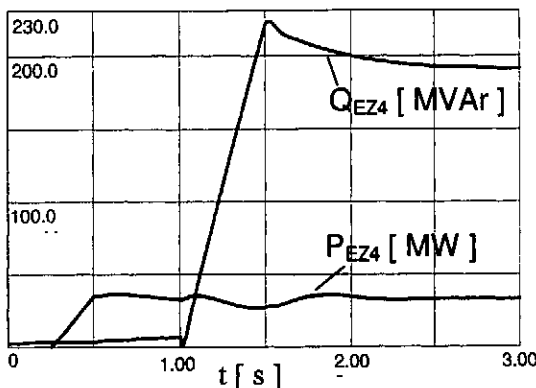
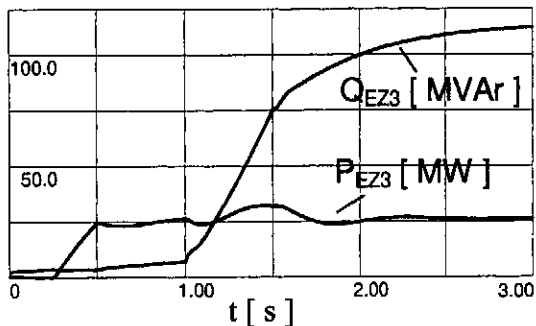


Fig. 8. Active and reactive power portions of generator EZ3 (above) and EZ4 (below)

angular speed shows that synchronous operation of generator EZ3 and EZ4 is provided during the considered time period. The busbar voltage verifies this statement. The system voltage is a three-phase system with a frequency of about 100 Hz. The calculated phase voltage shown in Fig. 9 has only minor deviations from its effective value of 6.06 kV. Voltage stability is provided although the load step in reactive power is two times higher than the one that can be achieved by means of the thyristor converters installed.

Investigations of a complete pulse (about 10 s) assuming different load cases and fault conditions will follow. Part of these investigations will be devoted to the effects of reactive power compensation (RPC) by switched capacitor banks.

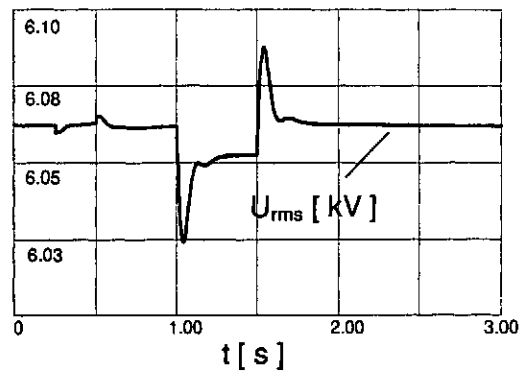


Fig. 9. Effective phase voltage in the 10.5 kV system

To compensate the inductive loads of the thyristor converters two 15 MVar RPC units were installed. An upgrade to 120 MVar is planned [6]. Switching up to eight RPC units during the coil ramp-up may additionally affect the dynamic stability of the two-generator system and must be investigated.

All results shall be compared to simulation results achieved by means of a "Watcom" ATP model allowing a more detailed modelling of saturation effects. Presently this work is in progress.

## V. CONCLUSION

For future experiments with elongated plasma flat-top phase it is favourable to feed the vertical field coils of ASDEX Upgrade by a parallel connection of the two flywheel generators EZ3 and EZ4.

The different machine parameters of the generators and the changeable load characteristics require extensive stability analyses in order to exclude potential hazards of a parallel connection.

First stability analyses employing the Simplorer code have shown that, as a matter of principle, a parallel operation of the generators EZ3 and EZ4 is possible.

However, the regulating parameters of the two-generator system must be adapted to the new conditions in order to operate the two-machine system with a balanced load distribution in the static and dynamic case and to meet the demands of safety standards.

Furthermore stability studies will be necessary to find the maximum load leading to instability under normal and fault conditions.

## VI. REFERENCES

- [1] M. Blaumoser, M. Kottmair, A. Wiczorek, O. Gruber, "ASDEX Upgrade power supply system", Proc. of 14<sup>th</sup> Symposium on Fusion Technology, Avignon, 1986, pp. 915-920

[2] SIMEC GmbH, "Simplorer", Version 4.0, Chemnitz, 1998

[3] G. Müller, "Grundlagen elektrischer Maschinen", Weinheim VCH Verlagsgesellschaft, 1994

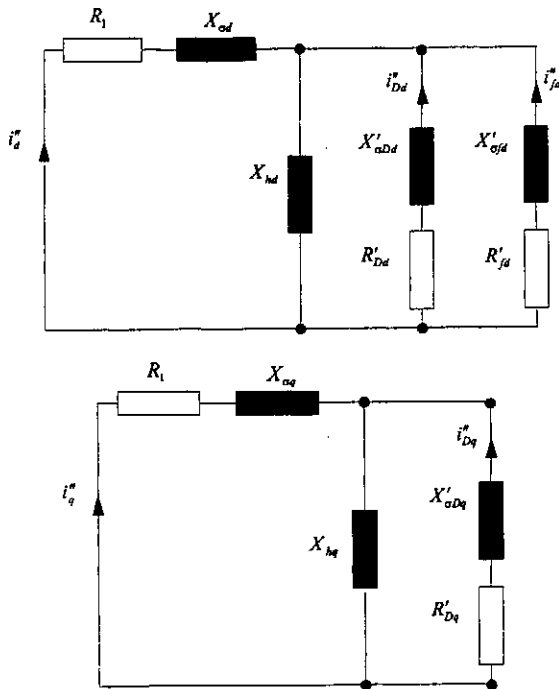
[4] G. Müller, "Theorie elektrischer Maschinen", Weinheim VCH Verlagsgesellschaft, 1994

[5] A. M. Miri, "Elektroenergiesysteme und Elektrische Anlagen", Vorlesungsbegleitendes Skriptum, Institut für Elektroenergiesysteme u. Hochspannungstechnik, Universität Karlsruhe, 1995

[6] C. Sihler, B. Streibl, R. Klein, W. Schlüter, M. Krohn, "Reactive Power Compensation for the Pulsed Power Supply of ASDEX Upgrade", Proc. of 20<sup>th</sup> Symposium on Fusion Technology, Marseille, 1998, pp. 887-890

### APPENDIX

The derivation of the dq0-parameters in equation system (1) was based on the leakage equivalent circuits shown in Figs. 10 and 11 [3-5].



$R'_{fd}$ : Direct axis component of exciter resistance  
 $R'_{Dd}$ : Direct axis component of damper resistance  
 $R'_{Dq}$ : Quadr. axis component of damper resistance

Fig. 10. Equivalent circuit for determining  $x_d''$  and  $x_q''$

Fig. 10 corresponds to equation system (2). The assumption that the short circuit time constant is initially dominated by the damper winding leads to equation system (3) for the subtransient time constants.

$$X'_d = X_{\sigma d} + X_{hd} \parallel \left( \frac{X'_{\sigma Dd} X'_{\sigma fd}}{X'_{\sigma Dd} X'_{\sigma fd}} \right) \quad (2)$$

$$X'_q = X_{\sigma q} + X_{hq} \parallel X'_{\sigma Dq}$$

$$X''_d = X_{\sigma d} + \frac{X_{hd} X_{\sigma d} X'_{\sigma fd}}{X_{hd} X'_{\sigma Dd} + X_{hd} X'_{\sigma fd} + X'_{\sigma Dd} X'_{\sigma fd}}$$

$$T''_d = \frac{X'_{\sigma Dd} + \frac{X_{hd} X_{\sigma d} X'_{\sigma fd}}{X_{hd} X'_{\sigma Dd} + X_{hd} X'_{\sigma fd} + X'_{\sigma Dd} X'_{\sigma fd}}}{\omega R'_{Dd}} \quad (3)$$

$$T''_q = \frac{X'_{\sigma Dq} + \frac{X_{hq} X_{\sigma q}}{X_{hq} + X'_{\sigma Dq}}}{\omega R'_{Dq}}$$

The equivalent circuit valid in the transient case (Fig. 11) delivers equations (4) and (5).

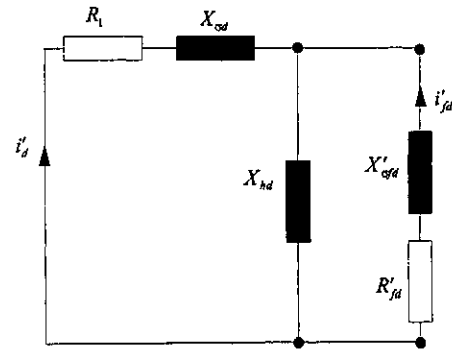


Fig. 11. Equivalent circuit for determination of  $x_d'$

$$X'_d = X_{\sigma d} + \frac{X_{hd} X'_{\sigma fd}}{X_{hd} + X'_{\sigma fd}} \quad (4)$$

$$T'_d = \frac{X'_{\sigma fd} + \frac{X_{hd} X_{\sigma d}}{X_{hd} + X'_{\sigma fd}}}{\omega R'_{fd}} \quad (5)$$

For EZ3 and EZ4 it can be assumed that  $X_{\sigma d} = X_{\sigma q} = X_{\sigma}$  and  $X_{\sigma Dd} = X_{\sigma Dq} = X_{\sigma D}$  so that the dq0-reactances can be calculated from the following equation system:

$$X_d = X_{hd} + X_{\sigma}$$

$$X_q = X_{hq} + X_{\sigma}$$

$$X''_d = X_{\sigma} + \frac{X_{hd} X'_{\sigma D} X'_{\sigma f}}{X_{hd} X'_{\sigma D} + X_{hd} X'_{\sigma f} + X'_{\sigma D} X'_{\sigma f}} \quad (6)$$

$$X''_q = X_{\sigma} + \frac{X_{hq} X'_{\sigma D}}{X_{hq} + X'_{\sigma D}}$$

$$X'_d = X_{\sigma} + \frac{X_{hd} X'_{\sigma f}}{X_{hd} + X'_{\sigma f}}$$

The assumption  $T_d'' = T_q''$  leads to a similar equation system for  $R_1$ ,  $R'_{Dd}$ ,  $R'_{Dq}$  and  $R'_{fd}$ .

Considering typical leakage coefficients and all relevant transformation ratios leads to the values of the dq0-parameters in equation system (1).